3588–3599 *Nucleic Acids Research, 2013, Vol. 41, No. 6* *Published online 8 February 2013*
doi:10.1093/nar/gkt073

DNA damage signaling induced by the G-quadruplex ligand 12459 is modulated by PPM1D/WIP1 phosphatase

Céline Douarre[1], Xénia Mergui[2], Assitan Sidibe[2], Dennis Gomez[3], Patrizia Alberti[2], Patrick Mailliet[2], Chantal Trentesaux[1,2,*] and Jean-François Riou[2,*]

[1]Laboratoire d'Onco-pharmacologie, JE 2428, Université de Reims, 51 rue Cognacq Jay, 51096 Reims cedex, France, [2]Structure des Acides Nucléiques, Télomères et Evolution, Inserm U565, CNRS UMR 7196, Muséum National d'Histoire Naturelle, 43 rue Cuvier 75231 Paris cedex 05, France and [3]Radiology and DNA repair group, Institut de Pharmacologie et de Biologie Structurale, CNRS UMR 5089, 205 route de Narbonne, 31077 Toulouse, France

Received April 5, 2012; Revised December 30, 2012; Accepted January 20, 2013

ABSTRACT

The triazine derivative 12459 is a potent G-quadruplex ligand that triggers apoptosis or delayed growth arrest, telomere shortening and G-overhang degradation, as a function of its concentration and time exposure to the cells. We have investigated here the DNA damage response induced by 12459 in A549 cells. Submicromolar concentrations of 12459 triggers a delayed Chk1-ATR–mediated DNA damage response associated with a telomeric dysfunction and a G2/M arrest. Surprisingly, increasing concentrations of 12459 leading to cell apoptosis induced a mechanism that bypasses the DNA damage signaling and leads to the dephosphorylation of Chk1 and γ-H2AX. We identified the phosphatase Protein Phosphatase Magnesium dependent 1D/Wild-type P53-Induced Phosphatase (PPM1D/WIP1) as a factor responsible for this dephosphorylation. SiRNA-mediated depletion of PPM1D/WIP1 reactivates the DNA damage signaling by 12459. In addition, PPM1D/WIP1 is activated by reactive oxygen species (ROS) induced by 12459. ROS generated by 12459 are sufficient to trigger an early DNA damage in A549 cells when PPM1D/WIP1 is depleted. However, ROS inactivation by *N*-acetyl cysteine (NAC) treatment does not change the apoptotic response induced by 12459. Because PPM1D expression was recently reported to modulate the recruitment of DNA repair molecules, our data would suggest a cycle of futile protection against 12459, thus leading to a delayed mechanism of cell death.

INTRODUCTION

Telomeres that cap chromosome ends are composed of tandem repeats of the sequence TTAGGGn with a 3′-single-stranded extension associated with proteins from the shelterin complex (1). This nucleoprotein structure is essential to avoid end of chromosomes to be recognized as a double-strand break by the DNA repair machinery and to trigger the DNA damage response (1). Two mechanisms have been reported in the maintenance of telomere length. The first requires telomerase to add TT AGGG repeats at the 3′-end (2). The second involves recombination between telomeres and is known as Alternative Lengthening of Telomeres (ALT) (3). Telomeres can fold into t-loop, a structure that may correspond to the invasion of the 3′-single-stranded extension into duplex DNA or into G-quadruplex DNA, a non-canonical four-stranded DNA structure based on the formation of guanine quartets.

G-quadruplexes are well-characterized conformations of sequences containing several repeats of guanines that arrange in guanine tetrads, stabilized by Hoogsteen hydrogen bounding and coordinated by central cations (4). Human telomeric sequence can form intramolecular G-quadruplexes showing an antiparallel conformation in sodium containing solutions or a parallel 'propeller' structure in potassium containing dehydrated solutions or in crystal (5).

*To whom correspondence should be addressed. Tel: +33 1 40 79 36 98; Fax: +33 1 40 79 37 05; Email: riou@mnhn.fr
Correspondence may also be addressed to Chantal Trentesaux. Tel: +33 1 40 79 36 98 Email: trentesaux@mnhn.fr
Present address:
Céline Douarre, Institut de Recherche en Immunologie et Cancérologie, Université de Montréal, Montreal, Quebec H3C 3J7, Canada.

Evidence is accumulating that G-quadruplexes can form among telomere repeats during lagging strand DNA replication and at the 3′-telomeric G-overhang (6). Although their existence in mammalian cells is based on indirect evidences (7), it has been demonstrated using specific antibodies that G-quadruplexes are formed in the macronuclei from ciliates (8). Further bioinformatic analysis of the human genome indicated the presence of thousand potential G-quadruplex-forming sequences (PQS) with a specific enrichment in regulatory regions such as gene promoters, UnTranslated Regions (UTRs) and splice sequences (9), suggesting a role for G-quadruplexes in the regulation of gene expression.

A strategy based on the interaction of small molecule ligands with telomeric G-quadruplex has emerged during the past decade (10). These compounds, also called telomere targeting agents, were initially derived from DNA intercalators and now present remarkable selective binding properties to G-quadruplex relative to duplex DNA (11). Several pieces of evidence suggest that these ligands are deleterious for the stability of telomeres in both telomerase positive and ALT tumor cell lines. These ligands are able to interfere directly with the binding of essential shelterin components, such as Protection Of Telomere 1 (POT1) and Telomeric Repeat Factor 2 (TRF2) in telomerase positive cell lines (6,10) or TRF2 and TopoIIIα in ALT cell lines (12). This action induces a DNA damage response and the evidence of telomere-dysfunction induced foci (TIFs) has been demonstrated for several G-quadruplex ligands (13–15). It must be noticed that these ligands also induced telomere-independent DNA damage foci that might be related to the presence of G-quadruplexes in other regions of the genome enriched in PQS (14,16,17) as evidenced recently for pyridostatin (18).

During telomere replication, the transient recruitment of DNA damage proteins is observed and controlled by the coordinating action of POT1 and TRF2 that, respectively, repress the ATR and ATM DNA damage signaling (19,20). A recent study suggests that the pentacyclic acridinium salt RHPS4 can interfere with telomere replication, triggering an ATR-dependent damage response pathway (15). In addition, ATR deficiency strongly sensitizes cells to the pyridine dicarboxamide derivative 360A and provokes telomere aberrations generated during telomere replication (21). In contrast, telomestatin does not affect telomere replication, as revealed by Co-FISH experiments in mouse embryonic fibroblast (22), but rather induces an ATM-dependent DNA damage response in human leukemia cell lines (23). Furthermore, 360A also triggers telomere aberrations in ATM-deficient cell lines (24).

These data suggested that the DNA damage response induced by G-quadruplex ligands may differ as a function of the chemical structure of the ligand or the nature of the cell line used. In addition, the cell proliferation defect also varies as a function of the ligand concentration used. Indeed, triazine derivatives trigger short-term (short-term corresponded to a treatment with 12459 for <72 h and long-term to a treatment with 12459 ≥8 days.) apoptosis (within 48–72 h) at high micromolar range concentrations (>5 μM) and a delayed growth arrest associated with a cell senescence phenotype in the low micromolar range concentrations after long-term treatment (25). The establishment of cell lines resistant to the triazine derivative 12459 by either progressive adaptation or by ethyl methyl sulfonate (EMS) mutagenesis also pointed out significant differences between short-term and long-term effects of the ligand (26,27). Cross resistance to other G-quadruplex ligands (telomestatin, Braco-19) is observed for the long-term senescence induction but is absent for short-term treatment (26,27). Some of the clones selected for resistance to 12459 also present an overexpression of the Bcl-2 protein, and A549 cells transfected by Bcl-2 display a resistance to the apoptotic action of 12459 (28). However, the Bcl-2 overexpression is not sufficient to confer resistance to the long-term effect of 12459, thus suggesting that 12459-directed senescence is uncoupled from apoptosis, a result that fits well with the differences of resistance mechanism obtained after short-term or long-term exposure with the ligand (28).

Here, we report that 12459 at submicromolar concentrations triggers a Chk1/ATR-mediated DNA damage response associated with G2/M arrest and telomeric dysfunction. However, using higher concentrations that induced apoptosis, 12459 triggers a mechanism that bypasses the DNA damage signaling and leads to the dephosphorylation of Checkpoint kinase 1 (Chk1). We identified the phosphatase Protein Phosphatase Magnesium dependent 1D/Wild-type P53-Induced Phosphatase (PPM1D/WIP1) as a factor responsible for this dephosphorylation. PPM1D/WIP1 is activated at early stage by reactive oxygen species (ROS) induced by 12459. ROS induced by 12459 correlated with the early activation of PPM1D/WIP1 but their scavenging by *N*-acetyl cysteine (NAC) do not modify the apoptotic response induced by 12459.

MATERIALS AND METHODS

Cell culture and drug treatment

Human A549 lung carcinoma cell line was obtained from the American Type Culture Collection (Rockville, MD, USA). Cells were cultured in Dulbecco's modified Eagle's medium (DMEM) with glutamax, supplemented with 10% fetal calf serum and 1% penicillin-streptomycin (Invitrogen) at 37°C in an atmosphere containing 5% CO_2.

For drug treatment, the triazine derivative 12459 (synthesized according to the patent WO-0140218) was dissolved in dimethylsulfoxide (DMSO) at 10 mM, and aliquots of this stock solution were kept at −20°C. Dilution to 1 mM was made in DMSO, and further dilutions were made in water. NAC (Sigma Aldrich) was dissolved in phosphate buffered saline (PBS) at 1 M and adjusted to pH 7.3 with sodium hydroxide.

For cell senescence experiments, A549 cells were seeded at 15 000/ml in 25 cm^2 culture dish. After 4 days of treatment, cells were trypsinized, counted and replated at 15 000/ml. At each passage, population doubling (PD) from untreated or 12459-treated cultures were calculated

according to the following formula: PD = Log Cell density Day 4 – Log 15 000/Log 2.

For siRNA experiments, A549 cells were plated in six-well culture plates at 1.5×10^5 cells/well in 2 ml DMEM without antibiotics. After 12 h, 100 nM siRNA were transfected for 4 h, using Lipofectamin 2000 (Invitrogen). Two days after transfection, cells were splitted at 1.5×10^5 cells/well in new culture dishes for two additional days. Four days after transfection, 12459, NAC or H_2O_2 were added for 4 h, and then treated cells were processed for western blotting or immunofluorescence experiments. The siRNA used here are: SiRNA PPM1D/WIP1: 5′-GGUUUCUCG UUGUCACC-3′, SiRNA control: 5′-UGCGCUACGAU GGACGAUG-3′.

Antibodies and western blot analysis

All experiments were performed with cells in a logarithmic phase by controlling the plating density. Cells were washed with ice-cold PBS and lysed in RIPA buffer [Tris–HCl 50 mM, pH 7.4, sodium desoxycholate 0.25%, NaCl 150 mM, ethylenediaminetetraacetic acid (EDTA) 1 mM, phenylmethylsulfonyl fluoride (PMSF) 1 mM] including a protease inhibitor cocktail at 1 μg/ml (Mini complete protease, Roche Diagnostics). After 30 min on ice, lysates were cleared by centrifugation. Protein concentration was quantified with the Bio-Rad protein assay. Cell lysates containing equal amounts of total protein (25–40 μg) were resolved on a 12% or 10% sodium dodecyl sulphate–polyacrylamide gel by electrophoresis, transferred to polyvinylidene fluoride (PVDF)-membrane (Macherey-Nagel) by electro-blotting in 25 mM Tris, pH 8.3, 192 mM glycine, 20% ethanol. Membranes were blocked for 3 h at room temperature in 10 mM Tris, pH 7.5, containing 0.15 M NaCl, 0.1% Tween 20 and 5% nonfat dry milk. Primary and secondary immunodetection, as well as washes, were performed in the same buffer using 5% dry milk. Western blot analysis was accomplished according to standard procedure using SuperSignal West Pico chemiluminescent substrate (Pierce). The following primary antibodies were used (1:1000 unless otherwise indicated): anti-phospho-histone (ser 139) γ-H2AX (Upstate), monoclonal anti-β-actin clone AC-15 (Sigma) (1:5000), anti-cleaved PARP asp 214 (Cell signaling), anti-P53 (Upstate), anti-phospho P53 Sampler Kit (Cell Signaling), anti P21 (BD Pharmingen), anti-Chk1, anti-phospho-Chk1(Ser317), anti-Chk2 and anti-phospho-Chk2 (Thr 68) (Cell Signaling), rabbit anti-PPM1D (BL 3066 Bethyl Laboratories).

Immunofluorescence

A549 cells were plated in six-well culture plates on glass coverslips. After drug treatment, cells were washed with PBS (pH 7.2), fixed with 4% paraformaldehyde and permeabilized with 20 mM Tris–HCl (pH 8.0), 50 mM NaCl, 3 mM $MgCl_2$, 300 mM sucrose and 0.5% v/v Triton X-100 for 15 min at room temperature. Cells were then washed twice with PBS (pH 7.2). Cells were blocked with 1% bovine serum albumin in PBS for 1 h and incubated with primary antibodies for 1–2 h at room temperature [1 ng/μl for TRF1 rabbit polyclonal ab1423 (Abcam) and/or 2 ng/μl for antiphospho γ-H2AX (Ser139) (Upstate)]. The nuclear DNA was stained with 1 μM of Hoechst 33342. After washing with PBS, proteins of interest were detected by incubation for 30 min with fluorescently labeled secondary antibodies (anti-mouse antibody labeled with Alexa 568 and anti-rabbit antibody labeled with Alexa 488 (Molecular Probes), then washed with PBS. The nuclear DNA was stained with 1 μg/ml Hoechst 33342 in PBS (pH 7.2) for 4 min. Cells were mounted in Shandon Immu-Mount medium (Thermo Scientific). Samples were observed with a DMR Leica microscope, and images were captured with a Cool Snap HQ camera (Roper Scientific) controlled by Metamorph software (Roper Scientific). Final images are composed of arithmetic stacks of 15–25 deconvoluted images, each 0.2 μM in z-step. Stacks of 15–30 images (16-bit grayscale) were acquired with a z-step of 0.2 μm with low illumination intensity.

ROS experiments

ROS production was determined using carboxy fluorescein-AM (CF) (Molecular Probes). After cell treatment, 5 μM CF was added for 30 min to the cell culture. Cells were then washed by PBS trypsinized and analyzed by spectrofluorimetry using 488 nm for excitation and 515 nm for fluorescent emission measurements. Results were normalized relative to untreated A549 cells, defined as 100%.

Flow cytometry

Cells were cultured in presence or absence of 1 μM of 12459. Cells were always seeded at the same density (7.5×10^5 cells/75 cm^2 flask) in the same medium volume (15 ml). At indicated time points, cells were harvested with trypsin and either seeded for the next time point or collected for subsequent cell cycle analysis. They were then washed in PBS containing 20 mM EDTA and fixed with 70% ethanol at −20°C.

When the experiment was completed, cells were collected by centrifugation, washed in PBS containing 20 mM EDTA and incubated in PBS containing 20 mM EDTA, 100 mg/ml RNase A (Sigma) and 20 mg/ml propidium iodide (Sigma) for 30 min at 37°C. Cell cycle analysis was assessed on a C6 Accuri flow cytometer (Becton Dickinson) and data treated with the FCS Express 4 software.

RESULTS

12459 induces a DNA damage response at telomeres associated with senescence

To evaluate whether 12459 triggers a DNA damage response in A549 cells, we have investigated the formation of DNA damage foci due to the presence of phosphorylated H2AX (γ-H2AX), a phosphorylated variant of histone 2A that associates with DNA double-strand breaks (29). Cells treated with increasing concentrations of 12459 (0.5, 1, 2 and 5 μM) for 4 days were analyzed by immunofluorescence for γ-H2AX-containing foci (Figure 1). Interestingly, a marked DNA damage

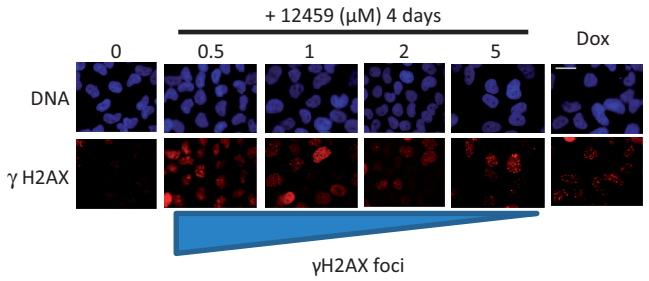

Figure 1. DNA damage response after 12459 treatment of A549 cells. Cells treated for 4 days with 0.5, 1, 2 and 5 μM 12459 or untreated were examined for γ-H2AX foci (red). Hoechst staining of DNA is shown in blue. As a positive control for DNA damage, A549 cells were treated with doxorubicin 0.5 μM for 24 h (Dox).

response was observed for low concentrations of 12459 (0.5 and 1 μM), while this DNA damage response is decreased using higher concentrations of 12459 (2 and 5 μM) (see later in the text). At low concentration conditions (0.5 and 1 μM for 4 days), 12459 induces a cell growth inhibition that precedes cell senescence, as no evidence of P21 expression was detected by western blotting (Figure 2A and B). Prolongation of 12459 treatment to 8 days provokes a cell growth arrest where P21 expression became readily detectable, suggesting the onset of cell senescence (Figure 2A and B).

To determine whether this 12459-induced DNA damage corresponds to damaged telomeres, A549 cells treated with 12459 (0.5 μM) for 8 days were analyzed for γ-H2AX-containing foci that co-localized with TRF1 (Figure 2C and Supplementary Figure S1). Results showed that DNA damage foci induced by 12459 co-localized with TRF1 and corresponded to TIFs (Telomere-dysfunction Induced Foci). TIFs were strongly increased [9.92 ± 8.34 (n = 38) TIFs/nuclei in treated cells, as compared with 3.17 ± 1.43 (n = 23) in control cells, $P < 0.001$], thus suggesting that 12459 induced a massive telomeric dysfunction associated with the onset of cellular senescence.

12459 triggers an ATR-mediated DNA damage response associated with G2/M arrest

To get further insight in the DNA damage checkpoint signaling associated with the cellular response to 12459-induced senescence, several effectors of ATM- or ATR-kinases have been evaluated. Results presented in Figure 2B indicate that 12459 treatment of A549 cells (0.5–2 μM) induces a transient overexpression of p53 after 4 days, with a slight activation of p53 at Ser 15 but without significant activation at Ser20. This activation of p53 disappears after 8 days during senescence. No obvious activation of Chk2(Thr68) was evidenced during 12459 treatment. In contrast, a significant activation of Chk1(Ser317) was found at the onset of senescence after 8 days that coincides with the expression of p21.

Cell cycle experiments were performed by fluorescence-activated cell sorting (FACS) in the presence or in the absence of the ligand (1 μM) and evaluated at days 3, 6, 9 and 13 (Figure 3). Results clearly indicated an effect of 12459 starting at day 6 corresponding to a G2/M accumulation together with a S phase decrease, in contrast to the G1/S arrest expected with replicative senescence (see

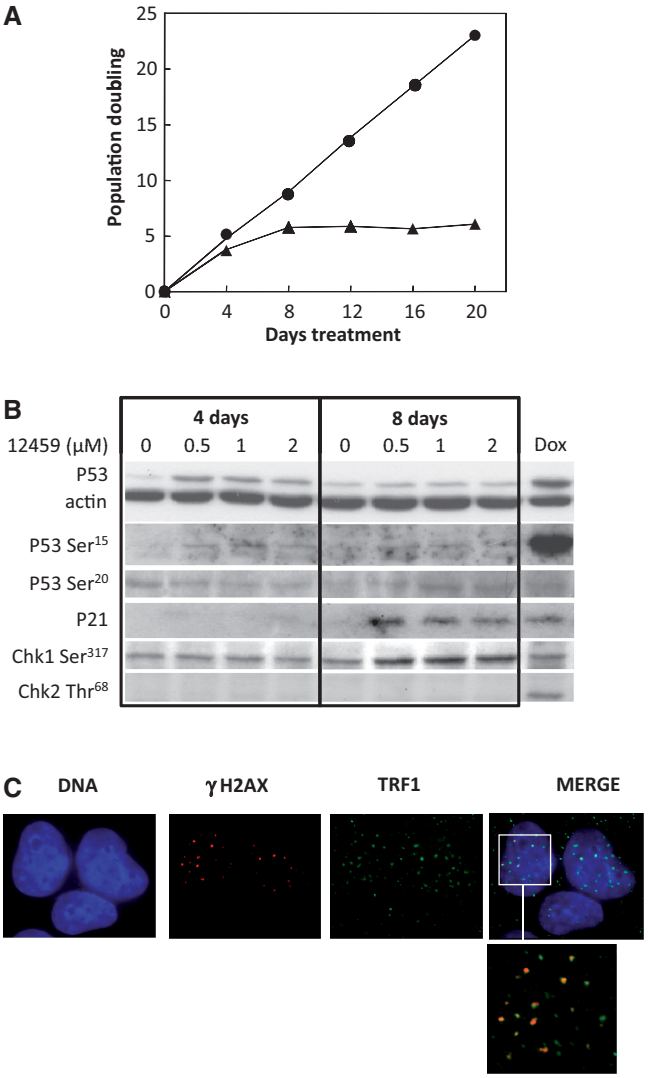

Figure 2. 12459 induced an ATR-mediated DNA damage response associated with senescence. (**A**) Long-term proliferation of A549 cells in the absence (closed circles) or presence (closed triangles) of 12459 (0.5 μM). A cell growth plateau at PD = 5 appears at day 8. (**B**) Western blot analysis of P53, P53 P-Ser 15, P53 P-Ser 20, P21, Chk1 P-Ser 317 and Chk2 P-Thr 68 protein expression in A549 cells untreated or treated with 12459 (0.5, 1 and 2 μM) for 4 days and 8 days. β-Actin was used as a control for protein loading, and doxorubicin 0.5 μM for 24 h (Dox) was used as a positive control for the DNA damage response. Ligand 12459 induced P21 expression and activation of Chk1 P-Ser 317 after 8 days of treatment. (**C**) A549 cells treated with 12459 (0.5 μM) for 8 days present γ-H2AX foci (red) that co-localized with TRF1 foci (green).

discussion). No evidence of sub-G1 accumulation was found, in agreement with the absence of apoptosis detectable in these conditions for 12459 (28).

Therefore, the DNA damage signaling induced by 12459 corresponds to a late involvement of the ATR-Chk1 pathway occurring at the onset of the growth arrest, which is consistent with a mechanism of telomere deprotection through POT1 targeting (7,30). Although a marked DNA damage was evidenced by γ-H2AX foci after 4 days, this damage does not lead to a significant signalization through Chk1 or Chk2, thus suggesting an unusual processing, as compared with classical DNA

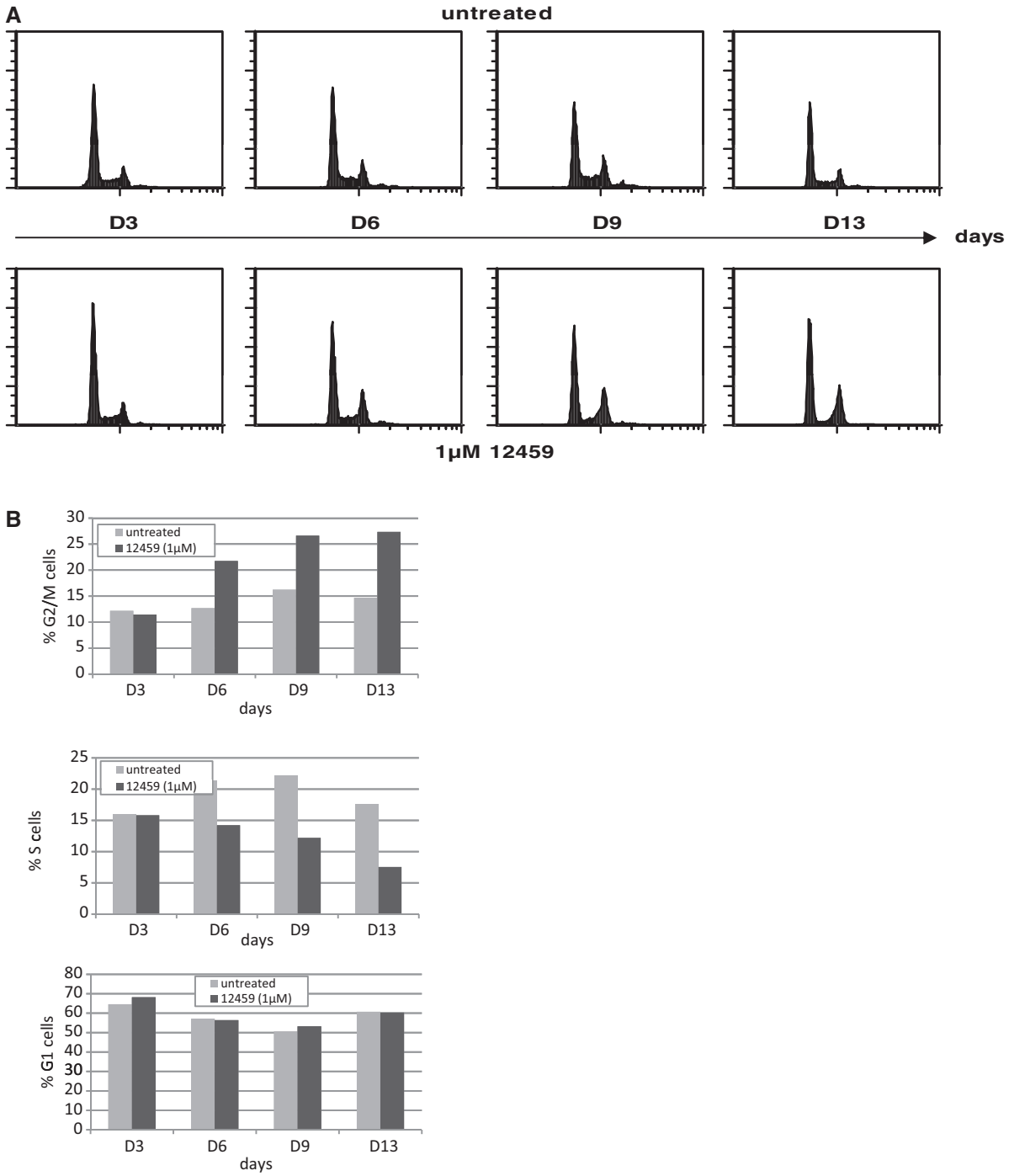

Figure 3. 12459 induced a G2/M accumulation associated with senescence. Delayed DNA damage signalization induced by 12459 in A549 cells. (**A**) A549 cells untreated or treated with 12459 (1 μM) for 3, 6 and 13 days were analyzed by FACS for cell cycle progression. (**B**) Quantifications of the percentage of cells in G2/M, S and G1 for the different conditions. Analysis was performed using the FSC Express 4 software.

damaging agents, such as doxorubicin that was used as a control in experiments presented in Figures 1 and 2 (0.5 μM, 24 h).

Pro-apoptotic concentration of 12459 induced a delayed DNA damage signalization

We previously reported that 12459 induces apoptosis after a 48 h delay for high drug concentrations (>5 μM) (25,28). In these conditions, the apoptotic pathway predominates over the appearance of senescent cells or growth-arrested cells. Surprisingly, we observed a marked dose-dependent decrease in the appearance of γ-H2AX foci in A549 cells under 12459 treatment (Figure 1). Only few A549 cells remain γ-H2AX positive in the presence of 12459 at 5 μM for 4 days and no positive γ-H2AX cells were detected using 10 μM 12459 for 4 days. Because these

concentrations induced a dramatic decrease in cell viability [see Figure 4 in (28)], it is possible that the apoptotic processes had eliminated cells presenting DNA damage. Therefore, we have examined the DNA damage induced by 12459 at early time treatment on A549 cells. The experiment presented in Figure 4A showed that A549 treatments with 12459 (10 and 20 μM) for 4 h and with 12459 (10 μM) for 24 h do not provoke any γ-H2AX foci, in contrast to 12459 (0.5 μM) for 8 days used as a positive control. In addition, a time-course western blot experiment (2–48 h) using 10 μM 12459 indicates that the ligand does not induce phosphorylation of γ-H2AX (data not shown). Interestingly, these data may suggest that 12459 treatment induces a dephosphorylation process.

When cellular extracts from the same experiment were blotted with Chk1(Ser317) antibodies, we also observed a dephosphorylation process, as compared with untreated control, that takes place between 2 and 4 h of drug treatment. Interestingly, a partial recovery of Chk1(Ser317) phosphorylation is observed at 8–16 h, that precedes a peak of p53 accumulation between 14 and 48 h corresponding to the onset of apoptosis (Figure 4B and data not shown, see also Supplementary Figure S2A). In these conditions, we do not observe any activation of the ATM-Chk2 signaling pathway because no phosphorylation of Chk2 was detected between 2 and 48 h (Figure 4B). These results are, however, consistent with the delayed apoptosis reported for this compound and suggest a mechanism that bypasses the DNA damaging signaling through the ATR-Chk1 pathway.

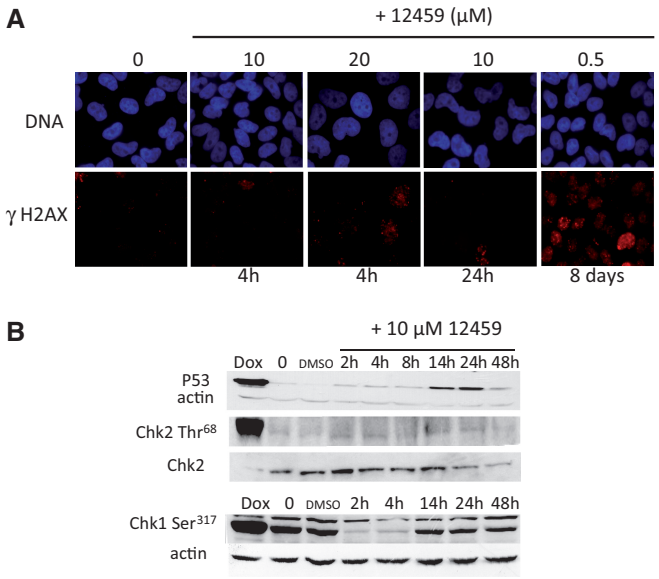

Figure 4. Delayed DNA damage signalization induced by 12459 in A549 cells. (**A**) Cells untreated or treated with 12459 for 4 h (10 and 20 μM) and for 24 h (10 μM) were examined for γ-H2AX foci (red). Hoechst staining of DNA is shown in blue. As a positive control for DNA damage, A549 cells were treated with 12459 (0.5 μM) for 8 days. (**B**) Western blot analysis of P53, Chk1 P-Ser 317, Chk2 and Chk2 P-Thr 68 protein expression in A549 cells untreated or treated with 12459 (10 μM) for the indicated times (2–48 h). β-Actin was used as a control for protein loading and doxorubicin 0.5 μM for 24 h (Dox) was used as a positive control for the DNA damage response.

12459 triggers p53 phosphorylation at Ser392 and induces p53 accumulation in nucleoli

Because p53 accumulation is detected at the onset of apoptosis, between 14 and 48 h after 12459 treatment, we wished to determine to which signaling pathway it corresponds. A549 cells treated for 24 h with 10 μM 12459 were blotted with different specific antibodies recognizing phorsphorylated serines at different positions (Ser 6, 9, 15, 20, 37, 46 and 392) and corresponding to different specific phosphorylation sites by kinases activated during the DNA damage signalization (Figure 5) (31). Interestingly, the only serine residue phosphorylated in response to 12459 treatment corresponded to Ser392 (Figure 5 and Supplementary Figure S2), known to be activated by ultraviolet (UV) light exposure or DNA-damaging anticancer agents, but not by gamma radiation (32). Some slight variations of reproducibility for p53 activation (between 14 and 48 h) were observed in the different experiments performed at these apoptotic concentrations that we attribute to the poor solubility of the compound at stock concentrations used for cell treatment (2 mM) to limit DMSO.

Data from literature indicated that p53 phosphorylation at Ser392 is also increased after p14ARF overexpression and is associated with p53 sequestration in nucleoli (33). Thus, we have investigated the nucleolar accumulation of p53 in 12459-treated A549 cells. As shown in Figure 6, 12459 treatment (10 μM for 24 h) induced a p53 accumulation in nuclei together with a nucleolar localization, in contrast to doxorubicin where p53 nuclear accumulation exclude nucleoli.

Altogether, our results indicate that 12459 triggers a specific phosphorylation of p53 at Ser392 together with

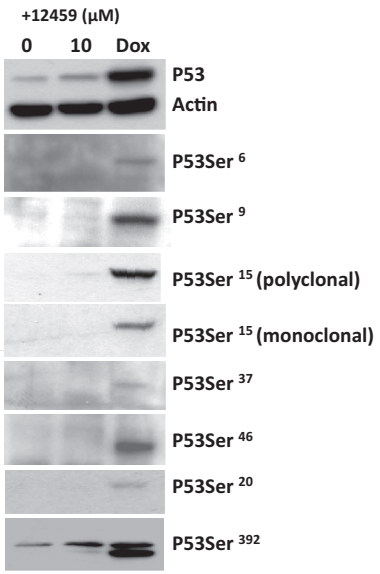

Figure 5. 12459 induces P53 phosphorylation at Ser 392. Western blot analysis of P53 and phosphorylation sites at Ser 6, 9, 15, 20, 37, 46 and 392 in A549 cells untreated or treated with 12459 (10 μM) for 24 h. β-Actin was used as a control for protein loading, and doxorubicin 0.5 μM for 24 h (Dox) was used as a positive control for the DNA damage response.

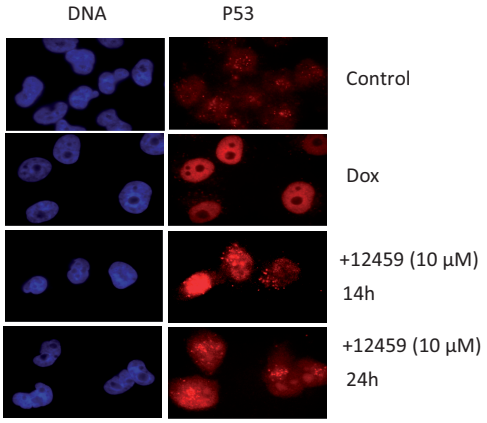

Figure 6. Nucleolar localization of P53 in A549 cells after 12459 treatment. Cells untreated or treated with 12459 (10 μM) for 14 h or 24 h were examined for P53 nuclear localization (red). Hoechst staining of DNA is shown in blue. As a positive control, cells were treated with (0.5 μM) doxorubicin for 24 h.

a nucleoli accumulation corresponding to an atypical situation, as DNA damaging agents such as doxorubicin or etoposide are able to induce p53 phosphorylation at multiple sites. Because p53 phosphorylation at Ser392 is a late process correlating with the onset of apoptosis or cell cycle sub-G2 accumulation (Supplementary Figure S6) and that Chk1 is transiently dephosphorylated at early times, we hypothesized that a phosphatase takes place in these processes.

12459-induced dephosphorylation of Chk1(Ser317) is associated with early PPM1D/WIP1 activation

PPM1D/WIP1 has been reported to dephosphorylate p53 and Chk1 during the activation of the DNA damage signaling mediated by ATR and to promote the dephosphorylation of γ-H2AX (34). Furthermore, PPM1D/WIP1 was also found to be activated by UV and ROS (35). These data suggest that PPM1D/WIP1 might be a good candidate to mask DNA damage signaling induced by 12459.

The expression of PPM1D/WIP1 was thus analyzed by western blot during the time-course induction of p53 by 12459 (Figure 7A). Results show that PPM1D/WIP1 expression is activated by 12459 treatment and starts after 2 h. An increased level of PPM1D/WIP1 is maintained up to 48 h (see also Supplementary Figure S3). Interestingly, the activation of PPM1D/WIP1 expression coincides with or precedes the dephosphorylation of Chk1(Ser317) occurring between 2 and 4 h of 12459 treatment (Figures 4B and 7A and Supplementary Figure S3). As a control, we also found the activation of PPM1D/WIP1, using conditions previously described to activate PPM1D/WIP1, i.e. UV irradiation (0.005 J/cm^2) or treatment with H_2O_2 (0.5 mM for 14 h).

PPM1D/WIP1 depletion reactivates DNA damage signaling by 12459

To further explore the function of PPM1D/WIP1, we used specific siRNA directed against PPM1D/WIP1 mRNA to decrease its protein expression (36). Transfection of A549 cells with siRNA-PPM1D indicated that in our experimental condition PPM1D protein levels were decreased to ~50% in both untreated and 12459-treated A549 cells, as compared with siRNA control (Figure 7B, see also Supplementary Figure S4). These conditions impaired PPM1D expression induced by H_2O_2 treatment. We next examined the effect of siRNA-PPM1D on the phosphorylation of Chk1(Ser317) after 12459 treatment (15 μM) for 4 h (Figure 7B, see also Supplementary Figure S4). Results showed that siRNA PPM1D treatment restore the phosphorylation of Chk1(Ser317), suggesting that PPM1D/WIP1 is responsible for the dephosphorylation. Indeed, we also observe a reactivation of γ-H2AX DNA damage foci induced by the siRNA directed against PPM1D in cells treated with 12459 (15 μM, 4 h) (Figure 7C). These results suggest that PPM1D/WIP1 is responsible for the inhibition of the ATR-Chk1 signaling pathway in the presence of apoptotic concentrations of 12459.

Reactive oxygen species are responsible for PPM1D/WIP1 activation but do not influence apoptosis induced by 12459

We have previously published that 12459 triggers a delayed apoptosis involving the mitochondrial pathway through alteration of Bcl2/Bax (28). However, we also observed that 12459 is able to trigger other rapid cellular events such as a decrease of the mitochondrial membrane potential and an increase of ROS within 2–4 h [see figure 3 in (28)]. We thus seek to determine the influence of ROS in PPM1D/WIP1 activation and 12459-mediated apoptosis. Treatment of A549 cells with H_2O_2 (0.5 mM) for 4 h reveals the presence of γ-H2AX foci (Figure 8). Interestingly, the DNA damage foci induced by H_2O_2 were found more pronounced when A549 cells were treated with siRNA against PPM1D than with siRNA controls, thus confirming that PPM1D is able to negatively regulate DNA damage induced by ROS. Interestingly, pretreatment of A549 cells with the ROS scavenger NAC (10 mM) is able to both protect A549 cells from DNA damage foci induced by H_2O_2 (Figure 8) and to decrease the activation of PPM1D induced by H_2O_2 (Figure 9A). Indeed, pretreatment of A549 cells with NAC is also able to counteract the induction of PPM1D by apoptotic concentration of 12459 (10 μM, 4 h) (Figure 9A). In these conditions, no γ-H2AX foci were observed (see NAC + 12459 in siRNA control cells in Figure 8). Interestingly, NAC treatment partially protects A549 cells from the DNA damage foci induced by 12459 when PPM1D/WIP1 is depleted by siRNA treatment, as only few figures of γ-H2AX positive cells remained (see NAC + 12459 in siRNA PPM1D-treated cells in Figure 8). These data suggested that ROS induced by 12459 are sufficient to induce an early DNA damage response when PPM1D/WIP1 is depleted by siRNA. Interestingly, we have also found that apoptosis induced by 12459 (10 μM, 48 h) in A549 cells was not affected by pretreatment of A549 cells by NAC (7.5 mM), as no modification of Poly-ADP-Ribose Polymerase (PARP) cleavage occurred during these conditions (Figure 9B). As a control, ROS production

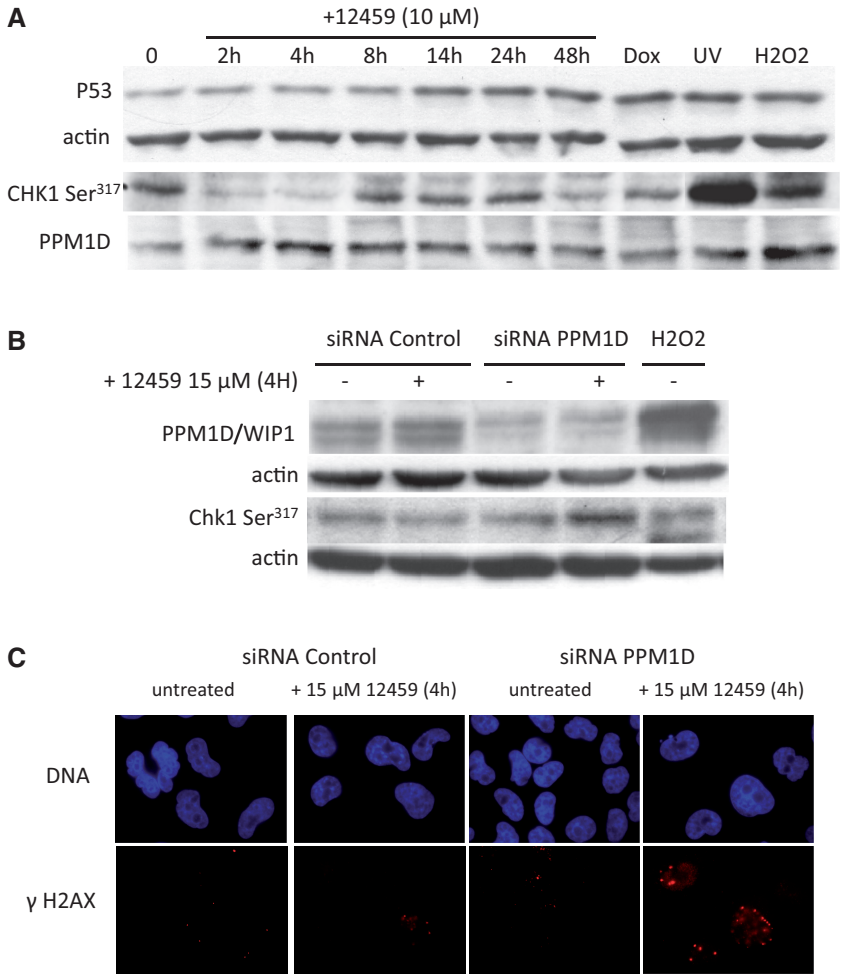

Figure 7. PPM1D/WIP1 is activated by 12459 and controls the DNA damage signaling by 12459 (**A**) Western blot analysis of PPM1D/WIP1, P53 and Chk1 P-Ser 317 protein expression in A549 cells untreated or treated with 10 μM 12459 for the indicated times (2–48 h). β-Actin was used as a control for protein loading, and doxorubicin 0.5 μM for 24 h (Dox) was used as a positive control for the DNA damage response, UV irradiation (0.005 J/cm^2) and H_2O_2 (0.5 mM for 14 h) were used as a positive control for the induction of PPM1D/WIP1. (**B**) Western blot analysis of PPM1D/WIP1 and Chk1 P-Ser 317 expression in A549 treated with siRNA control or siRNA PPM1D in the presence or absence of 12459 (15 μM, 4 h). H_2O_2 (0.5 mM for 4 h) was used as a positive control for the induction of PPM1D/WIP1. (**C**) Cells preatreated with siRNA control or siRNA PPM1D and untreated or treated with 12459 for 4 h (15 μM) were examined for γ-H2AX foci (red). Hoechst staining of DNA is shown in blue.

induced by 12459 was found decreased by NAC pretreatment (Figure 9C and Supplementary Table S1). In addition, 12459 or pretreatment with NAC does not alter telomere length by TRF analysis after 48 h treatment (Supplementary Figure S5). We conclude from these experiments that ROS induced at early stage (4 h) of 12459 treatment are able to activate the expression of PPM1D/WIP1 but do not participate to the apoptotic processes induced by 12459.

DISCUSSION

Our results suggest that submicromolar concentrations of 12459 induced the onset of 'senescence', as evidenced by a delayed growth inhibition and induction of SA-beta-galactosidase (25) together with the activation of p21 (this study), which is a figure already reported for different G-quadruplex ligands [i.e. BRACO-19 (37), see Supplementary Figure S7 for the chemical structures cited here] and a G2/M arrest. The onset of 'senescence' is also associated with the presence of DNA damage that mostly co-localized with telomere, suggesting that telomeric DNA is one of the cellular targets for 12459, in agreement with previous studies with G4 ligands (13–16). In addition, our study suggests that the DNA damage signaling response associated with 12459-induced senescence corresponds to the Chk1/ATR signaling pathway, thus suggesting that most of the damage are generated during DNA replication (38,39) and significantly differs from the replicative senescence induced in normal fibroblast cultures where the ATM signaling pathway was initially found predominant at shortened telomeres (40). Recent works challenged the current paradigm that the checkpoint response to eroded telomeres occurs primarily in G1/S (41,42). These reports also linked the post-replicative damage response at eroded telomeres to G2 arrest signaling in normal senescent cells. In addition, senescence in tumor cells may be driven at G2/M by DNA damage and is controlled by Chk1/P21

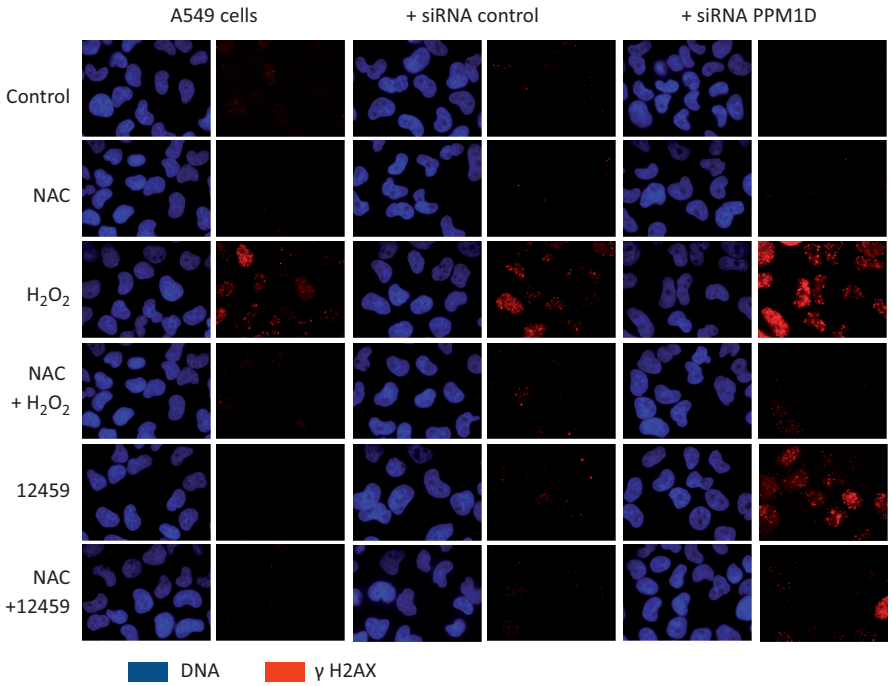

Figure 8. A549 cells transfected by siRNA control or by siRNA PPM1D were treated for 4 h with 12459 (15 μM) or with H_2O_2 (0.25 mM) in the presence or absence of NAC (10 mM) and examined for γ-H2AX foci (red). Hoechst staining of DNA is shown in blue. NAC protects A549 cells from the DNA damage induced by H_2O_2 and from the DNA damage induced by 12459 in the absence of PPM1D/WIP1.

when P53 is functional (42,43). In that case, arrested G2/M cells may enter a downstream senescence or undergo a mitotic catastrophe. Interestingly, our results indicated that 12459 triggers a G2/M arrest, in agreement with these recent findings.

The activation of Chk1/ATR by 12459 is in agreement with one of the proposed mechanisms of action of this class of compounds in which G-quadruplex stabilization blocks the binding of POT1 at G-overhang and/or at lagging strand during replication, leading to a replication stress with the accumulation of single-stranded DNA regions (7). Consistently, other G4 ligands, such as RHPS4 and pyridostatin, also induced a replication-dependent DNA damage response (17,18). An ATR-dependent ATM activation is also observed with RHPS4 (15), similar to that triggered by replication stress-inducing agents (44), and the DNA damage response induced by pyridostatin was found dependent on ATM, suggesting that the induction of DSB was mediated by mechanisms related to transcription-coupled repair (18). This contrasts with our results using 12459, where no evidence of Chk2 induction was found. This suggests subtle differences in the molecular pathways activated by these different G-quadruplex ligands that may be related to the nature of the cell line used for these studies. Alternatively, the nature of telomere deprotection (i.e. removal of POT1 and/or TRF2 from telomeres) may orient the nature of the DNA damage response to ATR and ATM pathways (30). It is noteworthy that telomestatin, which is able to trigger POT1 and/or TRF2 removal from telomeres, also triggers an ATM DNA damage response (14,23,45), while RHPS4 mostly removes POT1 from telomeres (15,17). However, all these G-quadruplex ligands, including 12459, do not present selectivity toward other potential DNA or RNA G-quadruplexes (46). Thus, we could not exclude that 12459 induced its DNA damage response through an alteration of TERRA transcription. Indeed, TERRA was found to facilitate ORC recruitment at telomeres, and its siRNA depletion induced telomeric aberrations, TIFs and loss of cell viability (47).

Another important finding of this study is the delayed DNA damage signaling associated with the induction of PPM1D/WIP1 phosphatase using pro-apoptotic concentrations of 12459. Our data indicate that 12459 induces an early activation of PPM1D/WIP1 and promotes the dephosphorylation of Chk1(Ser317) and γ-H2AX. WIP1 is a nuclear serine/threonine phosphatase of the PP2C family encoded by PPM1D gene (48) characterized by inhibitory functions on several tumor suppressor pathways, including p53 (49). PPM1D/WIP1 was initially reported to dephosphorylate proteins phosphorylated by the DNA damage-activated sensor kinases ATM, ATR and DNA-PK, such as Chk1, Chk2 and p53, thus reducing the cell cycle checkpoint activities and p53 stability (49). More recently, PPM1D/WIP1 was shown to interact with γ-H2AX and to mediate a delayed γ-H2AX dephosphorylation after DNA damage to promote the resolution of the DNA damage foci (50,51). The premature dephosphorylation of γ-H2AX after DNA damage by WIP1 expression also results in failure to recruit DNA repair molecules to DNA damage foci and attenuates the DNA damage response (52). PPM1D/WIP1 also maintains cellular competence to divide during an ongoing DNA damage response in G2 (53). This would explain the delayed apoptosis associated with the absence of DNA damage signaling triggered by 12459. At these

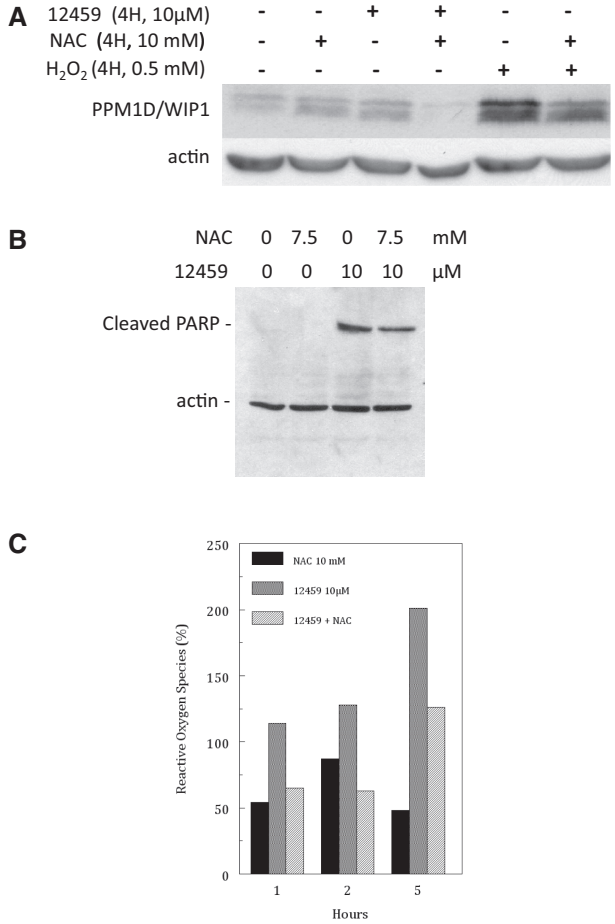

Figure 9. ROS are responsible for the activation of PPM1D/WIP1 by 12459 but do not influence apoptotic process. (**A**) Western blot analysis of PPM1D/WIP1 protein expression in A549 cells treated for 4 h with 12459 (10 μM) or H_2O_2 (0.5 mM) in the absence or presence of NAC (10 mM). NAC protects A549 cells from PPM1D activation induced by 12459 or H_2O_2. (**B**) Western blot analysis of cleaved-PARP protein expression in A549 cells treated for 48 h with 10 μM 12459 in the presence or absence of NAC (7.5 mM). β-Actin was used as a control for protein loading. (**C**) ROS were measured by spectrofluorimetry using CF probe in A549 cells treated for 1, 2 and 5 h with NAC (10 mM), 12459 (10 μM) or NAC (10 mM) and 12459 (10 μM), as indicated. Results were normalized relative to untreated A549 cells defined as 100%.

concentrations, 12459 induced a marked reduction of telomeric G-overhang (28) leading to enhanced telomeric dysfunction, the presence of sub-G2 cell population accumulating after 48 h of treatment (Supplementary Figure S6) that finally lead to cell death. In agreement, siRNA depletion of PPM1D/WIP1 restore the 12459-induced DNA damage signaling pathway, as evidenced by the early activation of Chk1(Ser 317) and γ-H2AX (Ser 139).

A late activation of p53 at Ser 392 together with p53 nucleolar accumulation was also observed under 12459 treatment. Such figure was already reported to occur preferentially in response to UV radiations or to treatment with cisplatin (32,54). Interestingly, a model in which p53(Ser392) accumulates was proposed when uncoupling between p53 accumulation and degradation occurs in response to various stimuli (55,56). Because PPM1D/WIP1 directly or indirectly dephosphorylates p53 at various residues, except at Ser392 (35,49), the late accumulation of p53 (Ser 392) and the lack of activation of p53 (Ser 6, 9, 15, 20, 37 and 46) may rather result from the accumulation of non-degradated forms of p53 than from an active signaling process.

Finally, our results indicated that ROS induced by 12459 treatment were responsible for the early activation of PPM1D/WIP1. Treatment of A549 cells with NAC decreased the activation of PPM1D/WIP1 by 12459 due to the early activation of ROS that was previously reported in the same cellular model (28). The production of ROS by 12459 was found to be dose-dependent (C. Douarre, unpublished data) and correlated with the dose-dependent decrease of γ-H2AX foci reported in this study (Figure 1). Because ROS have been shown to induce a DNA damage response at telomere (57), one may ask whether ROS induced by 12459 participates in the telomere deprotection effect. Our study indicates that at short-term (4 h) ROS triggered by 12459 are sufficient to induce a significant early DNA damage when PPM1D/WIP1 is partially depleted. In addition, NAC treatment strongly decreases the DNA damage response of 12459 when PPM1D/WIP1 is depleted. Because apoptosis at 48 h is not greatly affected by NAC treatment, it is tempting to conclude that PPM1D/WIP1 activation by 12459 provides enough protection to avoid a massive effect of ROS on telomeres but does not eliminate the damages induced by G-quadruplex formation at telomeres or in other G-rich parts of the genome. However, we cannot exclude that a combination between the direct effects of the compound at telomeres and indirect effects triggered by ROS is responsible for this cell death response, and future studies will aim to solve this issue. Another piece of evidence against the sole involvement of ROS in the telomeric effects of the ligand is provided by the study of the JFD9 resistant cell line to 12549 (26,28). This cell line was found resistant to the apoptotic effect of 12459 (10 μM) but not to the delayed growth arrest using submicromolar concentrations of 12459 (0.5–1 μM). In contrast to parental A549, 12459 (1 μM) does not induce the activation of ROS in JFD9 cells (C. Douarre, unpublished data).

In conclusion, our data suggest that ROS activation of PPM1D/WIP1 by 12459 in A549 cells may represent a mechanism of futile protection, leading to an inhibition of DNA repair signaling that further accumulates G-quadruplex-induced telomeric dysfunction or other genomic DNA damages but that finally lead to a delayed cell death.

SUPPLEMENTARY DATA

Supplementary Data are available at NAR Online: Supplementary Table 1 and Supplementary Figures 1–7.

FUNDING

'Ligue Nationale contre le Cancer, Equipe Labellisée 2010' and the Agence Nationale de la Recherche

[ANR-09-BLAN-0355 'G4 Toolbox' to J.F.R., P.A., P.M. and C.T.]. 'Ligue Nationale contre le Cancer' (doctoral fellowship to A.S.). Funding for open access charge: Institut national de la santé et de la recherche médicale.

Conflict of interest statement. None declared.

REFERENCES

1. O'Sullivan,R.J. and Karlseder,J. (2010) Telomeres: protecting chromosomes against genome instability. *Nat. Rev. Mol. Cell Biol.*, **11**, 171–181.
2. Martinez,P. and Blasco,M.A. (2011) Telomeric and extra-telomeric roles for telomerase and the telomere-binding proteins. *Nat. Rev. Cancer*, **11**, 161–176.
3. Cesare,A.J. and Reddel,R.R. (2010) Alternative lengthening of telomeres: models, mechanisms and implications. *Nat. Rev. Genet.*, **11**, 319–330.
4. Phan,A.T. (2010) Human telomeric G-quadruplex: structures of DNA and RNA sequences. *FEBS J.*, **277**, 1107–1117.
5. Haider,S.M., Neidle,S. and Parkinson,G.N. (2011) A structural analysis of G-quadruplex/ligand interactions. *Biochimie*, **93**, 1239–1251.
6. Bryan,T.M. and Baumann,P. (2011) G-Quadruplexes: from guanine gels to chemotherapeutics. *Mol. Biotechnol.*, **49**, 198–208.
7. De Cian,A., Lacroix,L., Douarre,C., Temime-Smaali,N., Trentesaux,C., Riou,J.F. and Mergny,J.L. (2008) Targeting telomeres and telomerase. *Biochimie*, **90**, 131–155.
8. Lipps,H.J. and Rhodes,D. (2009) G-quadruplex structures: in vivo evidence and function. *Trends Cell Biol.*, **19**, 414–422.
9. Huppert,J.L. (2010) Structure, location and interactions of G-quadruplexes. *FEBS J.*, **277**, 3452–3458.
10. Neidle,S. (2010) Human telomeric G-quadruplex: the current status of telomeric G-quadruplexes as therapeutic targets in human cancer. *FEBS J.*, **277**, 1118–1125.
11. Monchaud,D. and Teulade-Fichou,M.P. (2008) A hitchhiker's guide to G-quadruplex ligands. *Org. Biomol. Chem.*, **6**, 627–636.
12. Temime-Smaali,N., Guittat,L., Sidibe,A., Shin-ya,K., Trentesaux,C. and Riou,J.F. (2009) The G-quadruplex ligand telomestatin impairs binding of topoisomerase IIIalpha to G-quadruplex-forming oligonucleotides and uncaps telomeres in ALT cells. *PLoS One*, **4**, e6919.
13. Casagrande,V., Salvati,E., Alvino,A., Bianco,A., Ciammaichella,A., D'Angelo,C., Ginnari-Satriani,L., Serrilli,A.M., Iachettini,S., Leonetti,C. *et al.* (2011) N-cyclic bay-substituted perylene G-quadruplex ligands have selective antiproliferative effects on cancer cells and induce telomere damage. *J. Med. Chem.*, **54**, 1140–1156.
14. Gomez,D., Wenner,T., Brassart,B., Douarre,C., O'Donohue,M.F., El Khoury,V., Shin-ya,K., Morjani,H., Trentesaux,C. and Riou,J.F. (2006) Telomestatin-induced telomere uncapping is modulated by POT1 through G-overhang extension in HT1080 human tumor cells. *J. Biol. Chem.*, **281**, 38721–38729.
15. Rizzo,A., Salvati,E., Porru,M., D'Angelo,C., Stevens,M.F., D'Incalci,M., Leonetti,C., Gilson,E., Zupi,G. and Biroccio,A. (2009) Stabilization of quadruplex DNA perturbs telomere replication leading to the activation of an ATR-dependent ATM signaling pathway. *Nucleic Acids Res.*, **37**, 5353–5364.
16. Rodriguez,R., Muller,S., Yeoman,J.A., Trentesaux,C., Riou,J.F. and Balasubramanian,S. (2008) A novel small molecule that alters shelterin integrity and triggers a DNA-damage response at telomeres. *J. Am. Chem. Soc.*, **130**, 15758–15759.
17. Salvati,E., Leonetti,C., Rizzo,A., Scarsella,M., Mottolese,M., Galati,R., Sperduti,I., Stevens,M.F., D'Incalci,M., Blasco,M. *et al.* (2007) Telomere damage induced by the G-quadruplex ligand RHPS4 has an antitumor effect. *J. Clin. Invest.*, **117**, 3236–3247.
18. Rodriguez,R., Miller,K.M., Forment,J.V., Bradshaw,C.R., Nikan,M., Britton,S., Oelschlaegel,T., Xhemalce,B., Balasubramanian,S. and Jackson,S.P. (2012) Small-molecule-induced DNA damage identifies alternative DNA structures in human genes. *Nat. Chem. Biol.*, **8**, 301–310.
19. Palm,W. and de Lange,T. (2008) How shelterin protects Mammalian telomeres. *Annu. Rev. Genet.*, **42**, 301–334.
20. Verdun,R.E. and Karlseder,J. (2006) The DNA damage machinery and homologous recombination pathway act consecutively to protect human telomeres. *Cell*, **127**, 709–720.
21. Pennarun,G., Hoffschir,F., Revaud,D., Granotier,C., Gauthier,L.R., Mailliet,P., Biard,D.S. and Boussin,F.D. (2010) ATR contributes to telomere maintenance in human cells. *Nucleic Acids Res.*, **38**, 2955–2963.
22. Arnoult,N., Shin-ya,K. and Londono-Vallejo,J.A. (2008) Studying telomere replication by Q-CO-FISH: the effect of telomestatin, a potent G-quadruplex ligand. *Cytogenet. Genome Res.*, **122**, 229–236.
23. Tauchi,T., Shin-ya,K., Sashida,G., Sumi,M., Nakajima,A., Shimamoto,T., Ohyashiki,J.H. and Ohyashiki,K. (2003) Activity of a novel G-quadruplex-interactive telomerase inhibitor, telomestatin (SOT-095), against human leukemia cells: involvement of ATM-dependent DNA damage response pathways. *Oncogene*, **22**, 5338–5347.
24. Pennarun,G., Granotier,C., Hoffschir,F., Mandine,E., Biard,D., Gauthier,L.R. and Boussin,F.D. (2008) Role of ATM in the telomere response to the G-quadruplex ligand 360A. *Nucleic Acids Res.*, **36**, 1741–1754.
25. Riou,J.F., Guittat,L., Mailliet,P., Laoui,A., Renou,E., Petitgenet,O., Megnin-Chanet,F., Hélène,C. and Mergny,J.L. (2002) Cell senescence and telomere shortening induced by a new series of specific G-quadruplex DNA ligands. *Proc. Natl Acad. Sci. USA*, **99**, 2672–2677.
26. Gomez,D., Aouali,N., Londono-Vallejo,A., Lacroix,L., Megnin-Chanet,F., Lemarteleur,T., Douarre,C., Shin-ya,K., Mailliet,P., Trentesaux,C. *et al.* (2003) Resistance to the short term antiproliferative activity of the G-quadruplex ligand 12459 is associated with telomerase overexpression and telomere capping alteration. *J. Biol. Chem.*, **278**, 50554–50562.
27. Gomez,D., Aouali,N., Renaud,A., Douarre,C., Shin-ya,K., Tazi,J., Martinez,S., Trentesaux,C., Morjani,H. and Riou,J.F. (2003) Resistance to senescence induction and telomere shortening by a G-quadruplex ligand inhibitor of telomerase. *Cancer Res.*, **63**, 6149–6153.
28. Douarre,C., Gomez,D., Morjani,H., Zahm,J.M., O'Donohue,M.F., Eddabra,L., Mailliet,P., Riou,J.F. and Trentesaux,C. (2005) Overexpression of Bcl-2 is associated with apoptotic resistance to the G-quadruplex ligand 12459 but is not sufficient to confer resistance to long-term senescence. *Nucleic Acids Res.*, **33**, 2192–2203.
29. Rogakou,E.P., Pilch,D.R., Orr,A.H., Ivanova,V.S. and Bonner,W.M. (1998) DNA double-stranded breaks induce histone H2AX phosphorylation on serine 139. *J. Biol. Chem.*, **273**, 5858–5868.
30. de Lange,T. (2009) How telomeres solve the end-protection problem. *Science*, **326**, 948–952.
31. Lavin,M.F. and Gueven,N. (2006) The complexity of p53 stabilization and activation. *Cell Death Differ.*, **13**, 941–950.
32. Kapoor,M. and Lozano,G. (1998) Functional activation of p53 via phosphorylation following DNA damage by UV but not gamma radiation. *Proc. Natl Acad. Sci. USA*, **95**, 2834–2837.
33. Jackson,M.W., Agarwal,M.K., Agarwal,M.L., Agarwal,A., Stanhope-Baker,P., Williams,B.R. and Stark,G.R. (2004) Limited role of N-terminal phosphoserine residues in the activation of transcription by p53. *Oncogene*, **23**, 4477–4487.
34. Moon,S.H., Nguyen,T.A., Darlington,Y., Lu,X. and Donehower,L.A. (2010) Dephosphorylation of gamma-H2AX by WIP1: an important homeostatic regulatory event in DNA repair and cell cycle control. *Cell Cycle*, **9**, 2092–2096.
35. Takekawa,M., Adachi,M., Nakahata,A., Nakayama,I., Itoh,F., Tsukuda,H., Taya,Y. and Imai,K. (2000) p53-inducible wip1 phosphatase mediates a negative feedback regulation of p38 MAPK-p53 signaling in response to UV radiation. *EMBO J.*, **19**, 6517–6526.
36. Lu,X., Bocangel,D., Nannenga,B., Yamaguchi,H., Appella,E. and Donehower,L.A. (2004) The p53-induced oncogenic phosphatase PPM1D interacts with uracil DNA glycosylase and suppresses base excision repair. *Mol. Cell*, **15**, 621–634.

37. Incles,C.M., Schultes,C.M., Kempski,H., Koehler,H., Kelland,L.R. and Neidle,S. (2004) A G-quadruplex telomere targeting agent produces p16-associated senescence and chromosomal fusions in human prostate cancer cells. *Mol. Cancer Ther.*, **3**, 1201–1206.
38. Ward,I.M. and Chen,J. (2001) Histone H2AX is phosphorylated in an ATR-dependent manner in response to replicational stress. *J. Biol. Chem.*, **276**, 47759–47762.
39. Ward,I.M., Minn,K. and Chen,J. (2004) UV-induced ataxia-telangiectasia-mutated and Rad3-related (ATR) activation requires replication stress. *J. Biol. Chem.*, **279**, 9677–9680.
40. Herbig,U., Jobling,W.A., Chen,B.P., Chen,D.J. and Sedivy,J.M. (2004) Telomere shortening triggers senescence of human cells through a pathway involving ATM, p53, and p21(CIP1), but not p16(INK4a). *Mol. Cell*, **14**, 501–513.
41. Jullien,L., Mestre,M., Roux,P. and Gire,V. (2012) Eroded human telomeres are more prone to remain uncapped and to trigger a G2 checkpoint response. *Nucleic Acids Res.*, **41**, 900–911.
42. Lossaint,G., Besnard,E., Fisher,D., Piette,J. and Dulic,V. (2011) Chk1 is dispensable for G2 arrest in response to sustained DNA damage when the ATM/p53/p21 pathway is functional. *Oncogene*, **30**, 4261–4274.
43. Poehlmann,A., Habold,C., Walluscheck,D., Reissig,K., Bajbouj,K., Ullrich,O., Hartig,R., Gali-Muhtasib,H., Diestel,A., Roessner,A. *et al.* (2011) Cutting edge: Chk1 directs senescence and mitotic catastrophe in recovery from G(2) checkpoint arrest. *J. Cell Mol. Med.*, **15**, 1528–1541.
44. Stiff,T., Walker,S.A., Cerosaletti,K., Goodarzi,A.A., Petermann,E., Concannon,P., O'Driscoll,M. and Jeggo,P.A. (2006) ATR-dependent phosphorylation and activation of ATM in response to UV treatment or replication fork stalling. *EMBO J.*, **25**, 5775–5782.
45. Tahara,H., Shin-ya,K., Seimiya,H., Yamada,H., Tsuruo,T. and Ide,T. (2006) G-Quadruplex stabilization by telomestatin induces TRF2 protein dissociation from telomeres and anaphase bridge formation accompanied by loss of the 3′ telomeric overhang in cancer cells. *Oncogene*, **25**, 1955–1966.
46. Tran,P.L., Largy,E., Hamon,F., Teulade-Fichou,M.P. and Mergny,J.L. (2011) Fluorescence intercalator displacement assay for screening G4 ligands towards a variety of G-quadruplex structures. *Biochimie*, **93**, 1288–1296.
47. Deng,Z., Norseen,J., Wiedmer,A., Riethman,H. and Lieberman,P.M. (2009) TERRA RNA binding to TRF2 facilitates heterochromatin formation and ORC recruitment at telomeres. *Mol. Cell*, **35**, 403–413.
48. Fiscella,M., Zhang,H., Fan,S., Sakaguchi,K., Shen,S., Mercer,W.E., Vande Woude,G.F., O'Connor,P.M. and Appella,E. (1997) Wip1, a novel human protein phosphatase that is induced in response to ionizing radiation in a p53-dependent manner. *Proc. Natl Acad. Sci. USA*, **94**, 6048–6053.
49. Le Guezennec,X. and Bulavin,D.V. (2010) WIP1 phosphatase at the crossroads of cancer and aging. *Trends Biochem Sci.*, **35**, 109–114.
50. Moon,S.H., Lin,L., Zhang,X., Nguyen,T.A., Darlington,Y., Waldman,A.S., Lu,X. and Donehower,L.A. (2010) Wild-type p53-induced phosphatase 1 dephosphorylates histone variant gamma-H2AX and suppresses DNA double strand break repair. *J. Biol. Chem.*, **285**, 12935–12947.
51. Macurek,L., Lindqvist,A., Voets,O., Kool,J., Vos,H.R. and Medema,R.H. (2010) Wip1 phosphatase is associated with chromatin and dephosphorylates gammaH2AX to promote checkpoint inhibition. *Oncogene*, **29**, 2281–2291.
52. Cha,H., Lowe,J.M., Li,H., Lee,J.S., Belova,G.I., Bulavin,D.V. and Fornace,A.J. Jr (2010) Wip1 directly dephosphorylates gamma-H2AX and attenuates the DNA damage response. *Cancer Res.*, **70**, 4112–4122.
53. Lindqvist,A., de Bruijn,M., Macurek,L., Bras,A., Mensinga,A., Bruinsma,W., Voets,O., Kranenburg,O. and Medema,R.H. (2009) Wip1 confers G2 checkpoint recovery competence by counteracting p53-dependent transcriptional repression. *EMBO J.*, **28**, 3196–3206.
54. Wesierska-Gadek,J., Schloffer,D., Kotala,V. and Horky,M. (2002) Escape of p53 protein from E6-mediated degradation in HeLa cells after cisplatin therapy. *Int. J. Cancer*, **101**, 128–136.
55. Meek,D.W. and Cox,M. (2011) Induction and activation of the p53 pathway: a role for the protein kinase CK2? *Mol. Cell. Biochem.*, **356**, 133–138.
56. Cox,M.L. and Meek,D.W. (2010) Phosphorylation of serine 392 in p53 is a common and integral event during p53 induction by diverse stimuli. *Cell Signal.*, **22**, 564–571.
57. von Zglinicki,T., Saretzki,G., Ladhoff,J., d'Adda di Fagagna,F. and Jackson,S.P. (2005) Human cell senescence as a DNA damage response. *Mech. Ageing. Dev.*, **126**, 111–117.